

[Click here to view linked References](#)

1
2
3 **Assessment of early diastolic intraventricular pressure gradient in the left ventricle among**
4
5
6 **patients with repaired tetralogy of Fallot**
7

8
9
10
11
12 **Running head:** Early diastolic IVPG in repaired TOF
13
14
15
16
17

18
19 Maki Kobayashi, MDa; Ken Takahashi, MDa; Mariko Yamada, MDa; Kana Yazaki, MDa; Kotoko
20
21

22 Matsui, MDb; Noboru Tanaka, MDb; Sachie Shigemitsu, MDb; Katsumi Akimoto, MDb; Masahiko
23
24

25 Kishiro, MDb; Keisuke Nakanishi, MDc; Shihori Kawasaki, MDc; Masaki Nii, MDd; Keiichi Itatani,
26
27

28 MD, PhD; Toshiaki Shimizu, MD, PhDa
29
30
31
32
33
34

35 a Department of Pediatrics and Adolescent Medicine, Juntendo University, Graduate School of
36
37

38 Medicine, Tokyo, Japan
39
40

41 b Department of Pediatrics, Juntendo University, Faculty of Medicine, Tokyo, Japan
42
43

44 c Department of Cardiovascular Surgery, Juntendo University, Faculty of Medicine, Tokyo, Japan
45
46

47 d Department of Pediatric Cardiology, Shizuoka Children`s Hospital, Shizuoka, Japan
48
49

50 e Department of Cardiovascular Surgery, Cardiovascular Imaging Research Laboratory, Kyoto
51
52

53 Prefectural University of Medicine, Kyoto, Japan
54
55
56
57
58
59
60
61
62
63
64
65

1
2
3 **Author contributions:**
4

5
6 Article drafting, data collection/analysis/interpretation: Maki Kobayashi, MD
7

8
9 Study concept/design, critical revision of article, statistical analysis: Ken Takahashi, MD
10

11
12 Data collection/analysis/interpretation: Mariko Yamada, MD
13

14
15 Data collection/analysis/interpretation: Kana Yazaki, MD
16

17
18 Data collection/analysis/interpretation: Kotoko Matsui, MD
19

20
21 Data collection/analysis/interpretation: Noboru Tanaka, MD
22

23
24 Data collection/analysis/interpretation: Sachie Shigemitsu, MD
25

26
27 Data collection/analysis/interpretation: Katsumi Akimoto, MD
28

29
30 Study concept/design: Masahiko Kishiro, MD
31

32
33 Study concept/design: Keisuke Nakanishi, MD
34

35
36 Study concept/design: Shihori Kawasaki, MD
37

38
39 Study concept/design: Masaki Nii, MD
40

41
42 Study concept/design: Keiichi Itatani, MD, PhD
43

44
45 Critical revision of article: Toshiaki Shimizu, MD, PhD
46

47
48
49
50
51
52
53
54 **Corresponding author:** Ken Takahashi
55

56
57 Department of Pediatrics, Juntendo University, Graduate School of Medicine
58
59
60

1
2
3
4
5
6
7
8
9
10
11
12
13
14
15
16
17
18
19
20
21
22
23
24
25
26
27
28
29
30
31
32
33
34
35
36
37
38
39
40
41
42
43
44
45
46
47
48
49
50
51
52
53
54
55
56
57
58
59
60
61
62
63
64
65

2-1-1 Hongo, Bunkyo-ku, Tokyo 113-8421, Japan

Phone: +81-3-3813-3111; Fax: +81-3-5800-0216; E-mail: kentaka@juntendo.ac.jp

Abstract

Assessment of left ventricular (LV) dysfunction is vital in patients with repaired tetralogy of Fallot (rTOF). The early diastolic intraventricular pressure gradient (IVPG) in the LV plays an important role in diastolic function. IVPG is calculated as the intraventricular pressure difference divided by the LV length, which allows to account for differences in LV size and therefore calculate IVPG in children. We aimed to investigate the mechanisms of LV diastolic dysfunction by measuring mid-to-apical IVPG as an indicator of the active suction force sucking blood from the left atrium into the LV. We included 38 rTOF patients and 101 healthy controls. The study population was stratified based on age group into children (4–9 years), adolescents (10–15 years) and adults (16–40 years). IVPGs were calculated based on mitral inflow measurements obtained using color M-mode Doppler echocardiography. Although total IVPGs did not differ between rTOF patients and controls, mid-to-apical IVPGs in adolescents and adults were smaller among rTOF patients than among controls (0.15 ± 0.05 vs. 0.21 ± 0.06 mmHg/cm, $p < 0.05$; 0.09 ± 0.07 vs. 0.17 ± 0.05 mmHg/cm, $p < 0.001$; respectively). Additionally, only mid-to-apical IVPG correlated linearly with peak circumferential strain ($\rho = 0.217$, $p = 0.011$), longitudinal strain ($\rho = -0.231$, $p = 0.006$), torsion ($\rho = -0.200$, $p = 0.018$), and untwisting rate in early diastole ($\rho = -0.233$, $p = 0.006$). In rTOF, the mechanisms underlying diastolic dysfunction involve reduced active suction force, which correlates with reduced LV deformation in all directions.

1
2
3
4
5
6
7
8
9
10
11
12
13
14
15
16
17
18
19
20
21
22
23
24
25
26
27
28
29
30
31
32
33
34
35
36
37
38
39
40
41
42
43
44
45
46
47
48
49
50
51
52
53
54
55
56
57
58
59
60
61
62
63
64
65

Keywords: Tetralogy of Fallot; Intraventricular pressure gradient; Diastolic dysfunction;
Echocardiography

Introduction

In patients with repaired tetralogy of Fallot (rTOF), it is vital to detect left ventricular (LV) systolic dysfunction as early as possible, because LV dysfunction is one of the strongest determinants of poor clinical outcomes in these patients [1]. LV dysfunction is usually observed late after surgical correction of tetralogy of Fallot (TOF) [2], and its precise mechanisms remain unclear. Because ventricular diastolic dysfunction may predate systolic dysfunction and clinical symptoms [3], it is important to detect diastolic dysfunction both accurately and early. However, it is difficult to assess diastolic dysfunction in patients with rTOF by using conventional echocardiographic methods because such methods cannot distinguish the contribution of factors such as impaired myocardial relaxation, decreased recoil attributable to a stiffer ventricle, and dyssynchronous ventricular relaxation [4]; moreover, conventional echocardiographic measurements do not account for key features noted in patients with rTOF, including abnormal muscle structure, presence of an artificial patch, and abnormal pre- and after-load of ventricles [1, 3, 4].

The suction force that sucks blood from the left atrium (LA) into the LV during early diastole correlates with the tau index and represents the gold-standard indicator of diastolic function [5], where it plays a fundamental role [6-9]. This force is based on the intraventricular pressure difference (IVPD). While cardiac catheterization was previously necessary for measuring the IVPD, Greenberg et al. described a non-invasive method based on echocardiography [10]. Furthermore, assessment of IVPD in LV

1
2
3 segments (e.g., basal or mid-to-apical IVPD) has provided new and deep insight into the mechanisms
4
5
6 underlying diastolic function [6,9]. Specifically, mid-to-apical IVPD was found to be an indicator of
7
8
9 active suction force [6,9], which is more important when assessing diastolic function in a clinical
10
11
12 setting, while basal IVPD was mainly affected by LA pressure.[9] Despite the usefulness of segmental
13
14
15 IVPDs for the analysis of diastolic dysfunction [6,9,11], to the best of our knowledge, no previous
16
17
18 study has employed this approach for the assessment of diastolic function in patients with rTOF.
19
20
21

22 When cardiac function is assessed in the pediatric population, the size of the heart represents an
23
24
25 important issue to be considered, as the LV in adolescents and adults is almost twice as long as the LV
26
27
28 in infants. Popovic et al. demonstrated the effect of LV size on the magnitude of IVPD and
29
30
31 recommended the use of the intraventricular pressure gradient (IVPG) instead [12]. Since the IVPG is
32
33
34 calculated as the IVPD divided by the LV length, LV size can be accounted for, and cardiac function
35
36
37 can be accurately assessed in pediatric patients.
38
39
40

41 In the present study, we aimed to investigate the mechanistic details of LV diastolic dysfunction in
42
43
44 patients with rTOF. As our study included also pediatric patients, we used IVPG, rather than IVPD, to
45
46
47 assess diastolic dysfunction. Furthermore, we obtained and analyzed segmental IVPGs, with special
48
49
50 focus on mid-to-apical IVPG.
51
52
53
54
55
56
57
58
59
60
61
62
63
64
65

Materials and methods

We performed a prospective echocardiographic study of consecutive patients who visited the Department of Pediatrics at Juntendo University Hospital between May 2013 and September 2015.

The inclusion criteria were as follows: (1) rTOF, (2) age between 4 and 40 years, (3) normal sinus rhythm, (4) absence of chromosomal defects, and (5) absence of other systemic diseases. Data regarding the rTOF patients were compared with those regarding controls of within the same age and sex group. The controls were recruited from among non-cardiac patients (evaluated for non-cardiac chest pain or presenting with innocent cardiac murmurs) or local community volunteers examined at Juntendo University or Shizuoka Children's Hospital. The inclusion criteria for the controls were: no history of cardiovascular disease, normal sinus rhythm on electrocardiography, and normal echocardiographic findings. The study was approved by our local institutional review board. Written, informed consent for participation was obtained from all participants or their legal guardians.

Echocardiography

All subjects underwent full echocardiography performed using a GE Vivid E9 device (GE Healthcare, Milwaukee, WI, USA) equipped with an S6 or M5S probe. For each plane, three consecutive cardiac cycles were acquired while the participant held their breath at end-expiration. In younger children, we selected three cardiac cycles from the end-expiration phase. LV end-diastolic volume, end-systolic

1
2
3 volume, and ejection fraction were calculated with the modified Simpson method using the
4
5
6 measurements obtained in the apical two- and four-chamber views. The mitral inflow E-wave, A-wave,
7
8
9 E/A ratio, duration from the onset of the Q-wave to aortic valve closure, and mitral valve opening were
10
11
12 measured using pulse-wave Doppler. The peak myocardial velocities during early diastole (e') were
13
14
15 measured at the mitral lateral annulus by using tissue Doppler imaging. The pressure gradient at the
16
17
18 right ventricular outflow tract was estimated based on the peak continuous-wave Doppler velocity.
19
20
21
22 The right ventricular end-diastolic area, end-systolic area, and fractional area change were measured
23
24
25 as described in the relevant guidelines [13]. In addition, color M-mode measurements were obtained
26
27
28 using the apical four-chamber view [7,10]. Three LV short-axis planes at the basal, mid, and apical
29
30
31 levels were acquired at frame rates of 75–115 frames/s. For each plane, 3 consecutive cardiac cycles
32
33
34 were acquired and stored digitally for offline analysis using the EchoPAC system version 108.1.4 (GE
35
36
37
38 Healthcare, Milwaukee, WI, USA).

44 **Measurements of LV deformation**

45
46
47 The following parameters characterizing myocardial deformation were measured according to a
48
49
50 protocol described in detail elsewhere [14]: peak torsion, untwisting rate during early diastole, peak
51
52
53 circumferential strain, peak circumferential strain rate during early diastole, peak longitudinal strain,
54
55
56 and peak longitudinal strain rate during early diastole.
57
58
59
60

Measurements of IVPGs

For the measurement of IVPG, color M-mode images were analyzed with an in-house code written in MATLAB (The MathWorks, Natick, MA, USA) using the following image-processing algorithm

(Figure 1):

$$(\partial P)/(\partial s) = -\rho \cdot ((\partial v)/(\partial t) + v \cdot (\partial v)/(\partial s)) \quad (1)$$

The images were reconstructed using a de-aliasing technique. In Equation (1), P is the pressure, ρ is a constant representing the density of blood (1060 kg/m³), v is the transmitral flow velocity, s is the position along the scan line (i.e., a line along the transmitral flow where the color Doppler M-mode measurements were taken), and t is the time. The relative pressures within the region of interest can be calculated from the reconstructed velocity field [6]. At each point along the scan line, the relative pressure was expressed as the difference between the pressure at that position and the pressure at the position of the mitral annulus at aortic valve closure. By calculating the line integral along the scan line, the temporal profile of the LV apex pressure relative to the LA pressure was obtained. Subsequently, the peak IVPD from the mitral valvular annulus to the LV apex was calculated as described in detail elsewhere [6,7,10], via a protocol previously validated against direct measurements using micromanometers [7,10]. All data were measured from at least three beats, and the mean values were used for the final analysis. Because our study population included participants from three age groups and the LV length was almost twice as high in adults than in children, we calculated the IVPG

1
2
3 as IVPD divided by LV length [12].
4
5

6 The total IVPG was divided into the basal and mid-to-apical IVPG (Figure 2). The basal segment was
7
8 defined as the first third of the LV length from the mitral valve to the LV apex; the remaining segment,
9
10 defined as the first third of the LV length from the mitral valve to the LV apex; the remaining segment,
11
12 which measured two-thirds of the LV length, was defined as the mid-to-apical segment. We applied
13
14 this approach because some of our patients were children, and therefore the ventricular space could
15
16 only be divided using relative distances. For comparison, previous studies that included only adults
17
18 defined the basal segment as the first 2 cm from the mitral valve [6,9], which would have been
19
20 inappropriate in our pediatric participants. To quantify the characteristics of segmental IVPGs, the
21
22 values were expressed as percentages of segmental IVPG from the total IVPG (i.e., as basal IVPG/total
23
24 IVPG · 100 and mid-to-apical IVPG/total IVPG · 100).
25
26
27
28
29
30
31
32
33
34
35
36
37

38 **Grouping**

39
40

41 The study population was stratified according to age: the groups of children with (TOF1) or without
42
43 rTOF (Control1) included participants aged 4–9 years; the groups of adolescents with (TOF2) or
44
45 without rTOF (Control2) included participants aged 10–15 years; and the groups of adults with (TOF3)
46
47 or without rTOF (Control3) included participants aged 16–40 years.
48
49
50
51
52
53
54
55
56
57
58
59
60
61
62
63
64
65

Statistical analysis

All data are expressed as means \pm standard deviations. After evaluating data for normality, between-group differences were assessed using one-factor analysis of variance with a post hoc Tukey-Kramer comparison test for data with normal distributions or with the Steel-Dwass test for data with non-normal distributions. The correlation between IVPGs and each variable was evaluated using the Spearman correlation coefficient, which was expressed as ρ , as some values showed non-normal distributions. To estimate intra-observer reliability for IVPG measurements, randomly selected 5 patients and 5 controls were examined in the same manner. Two independent observers analyzed the same images, and one blinded observer repeated the analysis on a separate day. Bland-Altman limits of agreement analysis was used for assessing intra-observer and inter-observer reliability. Statistical significance was set at $p < 0.05$. Analyses were performed using JMP® version 8.1 (SAS Institute Inc., Cary, NC, USA).

Results

The baseline characteristics and results of the conventional echocardiographic measurements of the 38 patients with rTOF and 101 controls included in the study are listed in Table 1. The detailed characteristics of the patients who underwent rTOF are listed in Table 2. In terms of cardiac dysfunction, all patients were classified as having New York Heart Association functional class 1

1
2
3 without any clinical symptoms.
4
5
6
7

8
9 **IVPG measurements**
10

11
12 Representative data collected in normal controls and in patients with rTOF are shown in Figure 2. An
13
14 overview of the total and segmental IVPG measurements is provided in Figure 3 (see also
15
16 supplementary Table 1). Regarding the relationship between IVPG and age, the total IVPG did not
17
18 differ significantly between rTOF patients and controls. Although total IVPG was smaller in adults
19
20 with rTOF than in children with rTOF (TOF3 vs. TOF1), no such difference was noted among controls.
21
22 For each age group, basal IVPG was higher in patients with rTOF than in controls. However, there
23
24 was no significant difference in basal IVPG between patients with rTOF and controls when the data
25
26 for all age groups were pooled. The mid-to-apical IVPG in adolescents and adults were lower among
27
28 patients with rTOF than among controls (TOF2 vs. Control2; TOF3 vs. Control3; respectively).
29
30 Interestingly, mid-to-apical IVPG was lower in adults with rTOF than in children with rTOF (TOF3
31
32 vs. TOF1). The % of mid-to-apical IVPG was significantly smaller in patients with rTOF than in
33
34 controls for all age groups. Furthermore, the % of mid-to-apical IVPG was significantly smaller in
35
36 adults with rTOF than in children with rTOF (TOF3 vs. TOF1), although no such difference was noted
37
38 among controls. The % of basal IVPG was significant larger in patients with rTOF than in controls for
39
40 all age groups. Moreover, the % of basal IVPG was significantly larger in adults with rTOF than in
41
42
43
44
45
46
47
48
49
50
51
52
53
54
55
56
57
58
59
60
61
62
63
64
65

1
2
3 children with rTOF (TOF3 vs. TOF1), while no such difference was noted among controls.
4
5
6
7
8

9
10 **LV deformation parameters**

11
12 Myocardial deformation measurements are listed in table 3. Torsion and untwisting rate in absolute
13 values were significant smaller in children and adolescents with rTOF than in controls (TOF1 vs.
14 Control1; TOF2 vs. Control2, respectively). The absolute value of the circumferential strain in
15 adolescents was smaller among patients with rTOF than among controls (TOF2 vs. Control2). The
16 absolute value of longitudinal strain in both adolescents and adults was significant smaller in patients
17 with rTOF than in controls (TOF2 vs. Control2; TOF3 vs. Control3; respectively). In each age group,
18 neither the circumferential nor the longitudinal strain rate differed between patients with rTOF and
19 controls.
20
21
22
23
24
25
26
27
28
29
30
31
32
33
34
35
36
37
38
39
40

41 **Relationship between LV deformation and inflow parameters and IVPGs**

42 Both torsion and untwisting rate correlated only with mid-to-apical IVPG, and not with basal IVPG.
43
44 As the value of the untwisting rate was negative, the correlation coefficient between the untwisting
45 rate and mid-to-apical IVPG was negative. Similarly, circumferential and longitudinal strain correlated
46 only with mid-to-apical IVPG, and not with basal IVPG. As the values of these parameters were
47 negative, their correlation coefficient describing the relationship with mid-to-apical IVPG was
48
49
50
51
52
53
54
55
56
57
58
59
60
61
62
63
64
65

1
2
3 negative. On the other hand, the circumferential and longitudinal strain rates correlated mainly with
4
5
6 basal IVPG and total IVPG. The peak E and E/e' correlated with the total and basal IVPG, but not
7
8
9 with mid-to-apical IVPG.
10

11 12 13 14 15 16 **Intra- and inter-observer variabilities**

17
18
19 Bland–Altman analyses indicated excellent intra- and inter-observer reliabilities for the measurement
20
21
22 of total, basal, and mid-to-apical IVPG (Figure 4). Intra- and inter-observer reliabilities were excellent
23
24
25 for total, basal and mi-to-apical IVPG.
26
27
28
29
30

31 32 **Discussion**

33 34 35 **Mechanisms to create mid-to-apical IVPG**

36
37
38 Although the total IVPG did not differ significantly between patients with rTOF and controls,
39
40
41 segmental IVPG did. Therefore, it is worth to consider the role of each segment for diastolic function.
42

43
44 The first concern is which segment creates the active suction force, as this is an important part of
45
46
47 diastolic function [6,9] and it correlates with the tau index [8]. Previous reports have focused on
48
49
50 segmental IVPD in an effort to analyze the mechanisms underlying this force. Steine et al. [5] showed
51
52
53 that, in an experimental model of ischemia, the peak early diastolic IVPD was decreased only in the
54
55
56
57 apical portion, with abnormal LV motion, suggesting that the force acted only in the apical segment.
58
59
60

1
2
3 Several reports also suggested a similar mechanism of reduced suction force in the apical segment in
4
5
6 patients with diastolic dysfunction [5,6,15]. The second concern refers to the factors affecting the
7
8
9 magnitude of the suction force. The major determinant of diastolic suction is the elastic energy stored
10
11
12 during systole [16,17,18]. Nikolic et al. [16] showed that the suction volume from the LA to the LV
13
14
15 during diastole was directly related to the magnitude of the LV elastic recoil as a potential energy
16
17
18 stored during systole. As the circumferential and longitudinal strains represent the magnitude of LV
19
20
21 deformation, these parameters relate to the elastic recoil in the circumferential and longitudinal
22
23
24 directions, respectively. In our study, the values of the circumferential and longitudinal strains
25
26
27 correlated only with mid-to-apical IVPG, and not with basal IVPG. Based on the theories described
28
29
30 above, these correlations are considered to be very reasonable.
31
32

33
34
35 Besides the strain, torsional deformation is also considered to play an important role in LV diastolic
36
37
38 function to create active suction. Systolic torsional deformation is one of the mechanisms by which
39
40
41 potential energy is stored during ejection, in the form of a global LV “spring” [8]; this energy is
42
43
44 promptly released during the isovolumetric relaxation time and early diastole, and can be estimated as
45
46
47 the peak untwisting rate, which is proportional to the tau index and IVPD [8]. We found that the torsion
48
49
50 and untwisting rate were lower in rTOF patients than in controls, which is consistent with the findings
51
52
53 of previous studies [14, 15], and moreover showed a significant correlation with mid-to-apical IVPG.
54
55
56 Therefore, reduced torsional deformation is also considered an important causative factor of diastolic
57
58
59
60
61
62
63
64
65

1
2
3 dysfunction in rTOF.
4
5
6
7
8

9
10 **Mechanisms of elevation of basal IVPG**
11

12 Unlike mid-to-apical IVPG, basal IVPG was higher in rTOF patients than in controls for all age groups.
13
14

15 Patients with rTOF are speculated to have abnormal LV diastolic function with abnormally high E/e'
16
17

18 [4, 19], which is associated with elevated LA pressure [19]. Iwano et al. [9] concluded that, in patients
19
20

21 with diastolic heart failure, basal IVPD was preserved because of an increase in LA pressure, and this
22
23

24 basal IVPD maintained the peak E despite reduced LV suction. Our data showed that both E and E/e'
25
26

27 correlated only with basal IVPG, and not with mid-to-apical IVPG, suggesting that elevation of basal
28
29

30 IVPG in rTOF was indeed caused by elevated LA pressure. Although the LA pressure in patients with
31
32

33 diastolic dysfunction increases at the stage of reduced LV compliance, we noted that the absolute value
34
35

36 of IVPG was very small. Therefore, although our data may reflect elevated LA pressure, it is not clear
37
38

39 whether basal IVPG is clinically useful or not.
40
41
42
43
44
45
46

47 **Clinical implications**
48

49 In patients with TOF, the extent of LV deformation may decrease for a variety of reasons such as
50
51

52 pressure overload [14], volume overload of the right ventricle with unfavorable ventricular–ventricular
53
54

55 interactions [20], abnormal muscle fiber structure [21], duration and severity of preoperative cyanosis,
56
57
58
59
60
61
62
63
64
65

1
2
3 cardiopulmonary bypass, patching of the ventricular septal defect, myocardial fibrosis, and ventricular
4
5
6 dyssynchrony [2, 20-23]. Regarding LV deformation parameters and clinical outcomes in patients with
7
8
9 rTOF, Diller et al. recently showed that conventional echocardiographic parameters such as EF and
10
11
12 E/e' were not useful predictors, whereas longitudinal strain was one of the strongest predictors [1]. On
13
14
15 the contrary, Orwat et al. reported that, in younger patients with TOF, the strongest prognostic marker
16
17
18 was circumferential strain [24]. Therefore, it may be considered that the usefulness of circumferential
19
20
21 and longitudinal strains as indicators of clinical outcome has been confirmed.
22
23

24
25 The magnitude of the differences between rTOF patients and controls was much higher for mid-to-
26
27
28 apical IVPG than for longitudinal or circumferential strains. Specifically, relative to the values noted
29
30
31 in controls, mid-to-apical IVPG was 34% lower in adolescents and 50% lower in adults with rTOF,
32
33
34 whereas circumferential and longitudinal strains were only 17%–20% lower. This finding is likely
35
36
37 related to the fact that a decrease in ventricular deformation in any direction (i.e., circumferential strain,
38
39
40 longitudinal strain, and torsion) affects mid-to-apical IVPG, as suggested by the correlations we found
41
42
43 shown between mid-to-apical IVPG and LV deformation parameters. Therefore, compared to LV
44
45
46 deformation parameters, a reduced mid-to-apical IVPG may represent a be more sensitive indicator of
47
48
49
50
51 LV dysfunction and clinical outcomes.
52
53

54 55 56 57 **Limitations** 58 59 60

1
2
3 Several potential limitations should be considered. First, although the accuracy of echocardiography-
4
5
6 based measurement of IVPD has been validated by comparison to direct measurements using
7
8
9 micromanometers [7,20], such validation was not performed in studies involving human children.
10
11
12 However, the fundamental structure and motion of the LV are thought to be the same as those in the
13
14
15 models used for validation. Specifically, Popović et al. [12] showed the utility of IVPG data in small
16
17
18 animals, where the size of the heart is smaller than that in human infants. Therefore, the measurement
19
20
21 approach used in the present study is considered to be accurate. Second, as this study included a small
22
23
24 number of patients, the conclusions may be underpowered. Studies with a larger sample size are
25
26
27 needed before a robust conclusion can be put forth regarding the usefulness of mid-to-apical IVPD as
28
29
30 an early marker of LV dysfunction in patients with rTOF.
31
32
33

34 35 36 37 38 **Conclusions** 39 40

41 Regarding the mechanisms underlying LV diastolic dysfunction, our findings suggest that patients
42
43
44 with rTOF have reduced mid-to-apical IVPG, which indicates reduced active suction force related
45
46
47 with reduced LV deformation. The measurement of mid-to-apical IVPG may be useful for quantifying
48
49
50 diastolic dysfunction in patients with rTOF. These represent new insights regarding diastolic
51
52
53 dysfunction in patients with rTOF.
54
55
56
57
58
59
60
61
62
63
64
65

Acknowledgments

We thank the staff of Shizuoka Children's Hospital for collecting the echocardiographic data of children and adults with no cardiac defects (control group).

Compliance with ethical standards

Conflict of interest: The authors declare that there is no conflict of interests.

Ethical approval: All procedures performed in this study were in accordance with the ethical standards of the institutional and/or national research committee and with the 1964 Helsinki declaration and its later amendments or comparable ethical standards.

Informed consent: Informed consent was obtained from all individual participants included in the study, or from their legal representatives.

References

1. Diller GP, Kempny A, Liodakis E, Alonso-Gonzalez R, Inuzuka R, Uebing A, Orwat S, Dimopoulos K, Swan L, Li W, Gatzoulis MA, Baumgartner H (2012) Left ventricular longitudinal function predicts life-threatening ventricular arrhythmia and death in adults with repaired tetralogy of fallot. *Circulation* 125:2440-2446.
2. Geva T, Sandweiss BM, Gauvreau K, Lock JE, Powell AJ (2004) Factors associated with impaired clinical status in long-term survivors of tetralogy of Fallot repair evaluated by magnetic resonance imaging. *J Am Coll Cardiol* 43:1068-1074.
3. Nishimura RA, Tajik AJ (1997) Evaluation of diastolic filling of left ventricle in health and

1
2 disease: Doppler echocardiography is the clinician's Rosetta Stone. *J Am Coll Cardiol* 30:8-18.

3
4 4. Friedberg MK, Fernandes FP, Roche SL, Grosse-Wortmann L, Manlhiot C, Fackoury C,
5 Slorach C, McCrindle BW, Mertens L, Kantor PF (2012) Impaired right and left ventricular diastolic
6 myocardial mechanics and filling in asymptomatic children and adolescents after repair of tetralogy
7 of Fallot. *Eur Heart J Cardiovasc Imaging* 13:905-913.

8
9 5. Steine K, Stugaard M, Smiseth OA (1999) Mechanisms of retarded apical filling in acute
10 ischemic left ventricular failure. *Circulation* 99:2048-2054

11
12 6. Ohara T, Niebel CL, Stewart KC, Charonko JJ, Pu M, Vlachos PP, Little WC (2012) Loss
13 of adrenergic augmentation of diastolic intra-LV pressure difference in patients with diastolic
14 dysfunction: evaluation by color M-mode echocardiography. *JACC Cardiovasc Imaging* 5:861-870.

15
16 7. Yotti R1, Bermejo J, Antoranz JC, Desco MM, Cortina C, Rojo-Alvarez JL, Allué C, Martín
17 L, Moreno M, Serrano JA, Muñoz R, García-Fernández MA (2005) A noninvasive method for
18 assessing impaired diastolic suction in patients with dilated cardiomyopathy. *Circulation* 112:2921-
19 2929.

20
21 8. Notomi Y, Popovic ZB, Yamada H, Wallick DW, Martin MG, Oryszak SJ, Shiota T,
22 Greenberg NL, Thomas JD (2008) Ventricular untwisting: a temporal link between left ventricular
23 relaxation and suction. *Am J Physiol Heart Circ Physiol* 294:H505-513.

24
25 9. Iwano H, Kamimura D, Fox E, Hall M, Vlachos P, Little WC (2015) Altered spatial
26 distribution of the diastolic left ventricular pressure difference in heart failure. *J Am Soc Echocardiogr*
27 28:597-605.

28
29 10. Greenberg NL, Vandervoort PM, Firstenberg MS, Garcia MJ, Thomas JD (2001) Estimation
30 of diastolic intraventricular pressure gradients by Doppler M-mode echocardiography. *Am J Physiol*
31 *Heart Circ Physiol* 280:H2507-2515.

32
33 11. Stewart KC, Kumar R, Charonko JJ, Ohara T, Vlachos PP, Little WC. Evaluation of LV
34 diastolic function from color M-mode echocardiography. *JACC Cardiovasc Imaging* 4(1):37-46

35
36 12. Popović ZB, Richards KE, Greenberg NL, Rovner A, Drinko J, Cheng Y, Penn MS,
37 Fukamachi K, Mal N, Levine BD, Garcia MJ, Thomas JD (2006) Scaling of diastolic intraventricular
38 pressure gradients is related to filling time duration. *Am J Physiol Heart Circ Physiol* 291:H762-769.

39
40 13. Lang RM, Badano LP, Mor-Avi V, Afilalo J, Armstrong A, Ernande L, Flachskampf FA,
41 Foster E, Goldstein SA, Kuznetsova T, Lancellotti P, Muraru D, Picard MH, Rietzschel ER, Rudski L,
42 Spencer KT, Tsang W, Voigt JU (2015) Recommendations for cardiac chamber quantification by
43 echocardiography in adults: an update from the American Society of Echocardiography and the
44 European Association of Cardiovascular Imaging. *J Am Soc Echocardiogr* 28:1-39

45
46 14. Takayasu H1, Takahashi K, Takigiku K, Yasukochi S, Furukawa T, Akimoto K, Kishiro M,
47 Shimizu T (2011) Left ventricular torsion and strain in patients with repaired tetralogy of Fallot
48 assessed by speckle tracking imaging. *Echocardiography* 28:720-729.

15. van der Hulst AE, Delgado V, Holman ER, Kroft LJ, de Roos A, Hazekamp MG, Blom NA, Bax JJ, Roest AA (2010) Relation of left ventricular twist and global strain with right ventricular dysfunction in patients after operative "correction" of tetralogy of fallot. *Am J Cardiol* 106:723-729.
16. Nikolic SD, Yellin EL, Tamura K, Vetter H, Tamura T, Meisner JS, Frater RW (1988) Passive properties of canine left ventricle: diastolic stiffness and restoring forces. *Circ Res* 62:1210-1222.
17. Bell SP, Nyland L, Tischler MD, McNabb M, Granzier H, LeWinter MM (2000) Alterations in the determinants of diastolic suction during pacing tachycardia. *Circ Res* 87:235-240.
18. Solomon SB, Nikolic SD, Glantz SA, Yellin EL (1998) Left ventricular diastolic function of remodeled myocardium in dogs with pacing-induced heart failure. *Am J Physiol* 274(3 Pt 2):H945-954.
19. Koenigstein K1, Raedle-Hurst T, Hosse M, Hauser M, Abdul-Khaliq H (2013) Altered diastolic left atrial and ventricular performance in asymptomatic patients after repair of tetralogy of Fallot. *Pediatr Cardiol* 34:948-953.
20. van der Hulst AE1, Delgado V, Holman ER, Kroft LJ, de Roos A, Hazekamp MG, Blom NA, Bax JJ, Roest AA (2010) Relation of left ventricular twist and global strain with right ventricular dysfunction in patients after operative "correction" of tetralogy of fallot. *Am J Cardiol* 106:723-729.
21. Sanchez-Quintana D, Anderson RH, Ho SY (1996) Ventricular myoarchitecture in tetralogy of Fallot. *Heart* 76:280-286.
22. Babu-Narayan SV, Kilner PJ, Li W, Moon JC, Goktekin O, Davlouros PA, Khan M, Ho SY, Pennell DJ, Gatzoulis MA (2006) Ventricular fibrosis suggested by cardiovascular magnetic resonance in adults with repaired tetralogy of fallot and its relationship to adverse markers of clinical outcome. *Circulation* 113:405-413.
23. Hausdorf G, Hinrichs C, Nienaber CA, Schark C, Keck EW (1990) Left ventricular contractile state after surgical correction of tetralogy of Fallot: risk factors for late left ventricular dysfunction. *Pediatr Cardiol* 11:61-68.
24. Orwat S, Diller GP, Kempny A, Radke R, Peters B, Kühne T, Boethig D, Gutberlet M, Dubowy KO, Beerbaum P, Sarikouch S, Baumgartner H and German Competence Network for Congenital Heart Defects Investigators (2016) Myocardial deformation parameters predict outcome in patients with repaired tetralogy of Fallot. *Heart* 102: 209-215.

Figure Legends

1
2
3
4
5
6
7
8
9
10
11
12
13
14
15
16
17
18
19
20
21
22
23
24
25
26
27
28
29
30
31
32
33
34
35
36
37
38
39
40
41
42
43
44
45
46
47
48
49
50
51
52
53
54
55
56
57
58
59
60
61
62
63
64
65

Figure 1. Calculation of the intraventricular pressure gradient (IVPG). From the four-chamber view showing mitral inflow (a), the corresponding color M-mode Doppler image is captured (b) with the cursor parallel to the mitral inflow in an apical four-chamber view. The zero line of the Nyquist limit for two-dimensional color Doppler imaging is placed on the lower edge of the scale, and the Nyquist limit was set at 30% above the peak E wave velocity to mitigate the aliasing phenomenon. Euler's equation, shown in Equation (1), was used to calculate the intraventricular pressure difference at each point. A three-dimensional temporal and spatial profile of the IVPG is generated (c). Subsequently, the total IVPG (d) and segmental IVPGs (e) in early diastole are identified.

Figure 2. Examples of intraventricular pressure gradients (IVPGs) in normal controls (a to d) and in patients with rTOF (e to h). In normal controls, the mid-to-apical IVPG is maintained (d). However, the IVPG decreased rapidly in the basal segments, and a reduced mid-to-apical IVPG was observed in rTOF patients with very small apical IVPG (h).

rTOF = repaired tetralogy of Fallot; AoV = Aortic valve

Figure 3. Box plots of the distribution of values for intraventricular pressure differences and gradients. The study population was composed of TOF patients and normal controls, and was stratified according

1
2
3 to age group as follows: TOF1 and Control1, 4–9 years; TOF2 and Control2, 10–15 years; and TOF3
4
5
6 and Control3, 16–40 years. * $p < 0.05$ and ** $p < 0.001$ refer to comparisons between TOF and controls
7
8
9 from the same age group; † $p < 0.05$ and refer to comparisons between TOF1 and TOF2 or TOF3, or
10
11
12 between Control1 and Control2 or Control3.
13

14
15
16 IVPG = intraventricular pressure gradient
17
18
19
20
21

22 Figure 4. Bland-Altman plots depicting intraobserver and interobserver reliability for the measurement
23
24
25 of = intraventricular pressure gradient (IVPG) values. Total IVPG (a, b), basal IVPG (c, d), and mid-
26
27
28 to-apical IVPG (e, f) were measured in 10 subjects.
29
30

31 IVPG = intraventricular pressure gradient
32
33
34
35
36
37
38
39
40
41
42
43
44
45
46
47
48
49
50
51
52
53
54
55
56
57
58
59
60
61
62
63
64
65

Table 1						
Baseline characteristics and basic measurements						
	TOF 1 (n=12)	TOF 2 (n=13)	TOF 3 (n=13)	Control 1 (n=32)	Control 2 (n=33)	Control 3 (n=36)
Age (y)	7.0 ± 1.3	13.0 ± 1.2 †	24.2 ± 7.1 † † §§	7.7 ± 1.3	12.4 ± 1.3 ††	25.7 ± 5.4 †† §§
Male / Female	6/6	8/5	4/9	19/12	17/16	18/18
Body Height (cm)	115 ± 9	153 ± 8 ††	160 ± 11 ††	122 ± 9	151 ± 8 ††	166 ± 9 †† §§
Body Weight (kg)	19.3 ± 4.0	46.8 ± 11.2 ††	56.3 ± 8.4 †† §	24.1 ± 4.5	43.8 ± 7.4 ††	59.8 ± 10.9 †† §§
Body surface area (m ²)	0.79 ± 0.11	1.41 ± 0.19 ††	1.58 ± 0.15 ††	0.90 ± 0.11	1.36 ± 0.13 ††	1.66 ± 0.19 †† §§
Heart rate (bpm)	81.0 ± 15.9	69.0 ± 7.1 †	58.3 ± 8.0 †† §	76.1 ± 10.4	69.7 ± 10.8	61.2 ± 8.1 †† §
Systolic blood pressure (mmHg)	94.7 ± 7.0	99.2 ± 12.6	113.8 ± 11.6 ††§	99.9 ± 9.3	106.2 ± 9.9 ††	118.1 ± 12.0 ††
Diastolic blood pressure (mmHg)	50.0 ± 6.9	55.8 ± 6.8 ††	66.1 ± 9.9 ††	54.0 ± 8.3	59.0 ± 9.2 ††	70.1 ± 9.6 †† §§
LV Length (cm)	5.71 ± 0.57	7.54 ± 0.51 ††	7.62 ± 0.63 ††	5.78 ± 0.51	7.10 ± 0.63 ††	7.90 ± 0.78 †† §§
LV EDV/BSA (ml/m ²)	46.4 ± 6.9	52.4 ± 17.2	45.8 ± 8.4	44.5 ± 9.7	46.6 ± 12.6	49.0 ± 14.6
LV ESV/BSA (ml/m ²)	15.6 ± 2.5	17.3 ± 6.6	16.3 ± 4.2	14.9 ± 4.4	15.5 ± 4.8	17.9 ± 5.9
LV ejection fraction (%)	66.1 ± 3.3	67.6 ± 4.2	64.4 ± 5.7	66.7 ± 3.7	66.9 ± 4.0	63.3 ± 4.5 † §

E (m/sec)	1.20 ± 0.20 *	1.29 ± 0.10 **	1.01 ± 0.23 † §§	1.02 ± 0.13	1.07 ± 0.17	0.91 ± 0.14 §
A (m/sec)	0.50 ± 0.18	0.44 ± 0.08	0.44 ± 0.08	0.45 ± 0.09	0.50 ± 0.13	0.48 ± 0.10
E/A ratio	2.71 ± 1.12 **	2.97 ± 0.72 *	2.42 ± 0.70	2.34 ± 0.57	2.24 ± 0.55	1.98 ± 0.55
e' lateral (cm/sec)	14.4 ± 3.9*	17.2 ± 4.8	15.1 ± 3.1	18.9 ± 2.4	18.8 ± 3.4	18.0 ± 2.8
E/e' ratio	9.20 ± 3.92 **	8.09 ± 2.37 *	6.93 ± 2.03 * †	5.48 ± 1.01	5.83 ± 1.22	5.13 ± 0.94
RV EDA/BSA (cm ² /m ²)	14.8 ± 4.0 **	14.1 ± 3.1 *	11.4 ± 1.7 *	10.5 ± 2.9	10.1 ± 3.6	7.9 ± 2.6 † §
RV ESA/BSA (cm ² /m ²)	6.7 ± 3.1	6.6 ± 1.8	5.3 ± 1.3	5.0 ± 1.8	5.0 ± 2.2	3.8 ± 1.7
RV Fractional Area Change (%)	55.7 ± 11.3	53.2 ± 7.2	53.1 ± 8.9	53.1 ± 9.1	52.5 ± 8.1	52.7 ± 9.0
TAPSE (mm)	14.7 ± 3.4 **	16.3 ± 2.9 **	15.6 ± 3.0 **	19.2 ± 2.1	21.0 ± 3.9	21.5 ± 2.7 †
MAPSE (mm)	14.0 ± 3.0	15.8 ± 2.5	14.7 ± 2.7	13.0 ± 1.9	14.5 ± 2.0 †	14.7 ± 1.6

TOF = Tetralogy of Fallot; LV = left ventricle; EDV = end diastolic volume; ESV = end systolic volume; BSA = body surface area; RV = right ventricle; EDA = end diastolic area; ESA = end systolic area;

The study population was composed of TOF patients and normal controls, and was stratified according to age group as follows: TOF1 and Control1, 4–9 years; TOF2 and Control2, 10–15 years; and TOF3 and Control3, 16–40 years. *p < 0.05 and **p < 0.001 refer to comparisons between TOF and controls from the same age group; † p < 0.05 and † † p < 0.001 refer to comparisons between TOF1 and TOF2 or TOF3, or between Control1 and Control2 or Control3; § p < 0.05 and § § p < 0.001 refer to comparisons between TOF2 and TOF3, or between Control2 and Control3.

Table2			
Patient Characteristics			
	TOF 1 (n=12) 4-9y	TOF 2 (n=13) 10-15 y	TOF 3 (n=12) ≥ 16 y
Age at repair (year)	1.5 ± 0.5	1.4 ± 0.5	2.6 ± 1.2
Duration from the repair (year)	5.5 ± 1.5	11.7 ± 1.2	21.6 ± 6.3
Transannular patch (TAP), n (%)	8 ()	9 ()	8 (66.7)
Non transannular patch, n (%)	4 (33.3)	1 (7.7)	5(41.7)
Rastelli , n (%)	0 (0)	3 (23.1)	0 (0)
previous shunt palliation, n (%)	5 (41.7)	3 (23.1)	4 (33.3)
Pulmonary regurgitation ≥ moderate, n (%)	9 (75.0)	9 (69.2)	8 (66.7)
RVOT pressure gradient (mmHg)	17.8 ± 13.9	28.7 ± 12.4	21.2 ± 9.7
QRS duration (msec)	124 ± 24	121 ± 27	134 ± 35
NYHA class ≥ II (%)	0	0	0

TOF = Tetralogy of Fallot; RVOT = right ventricular outflow tract; NYHA = New York Heart Association

Table 3						
Myocardial deformation measurements						
	TOF 1 (n=12)	TOF 2 (n=13)	TOF 3 (n=13)	Control 1 (n=32)	Control 2 (n=33)	Control 3 (n=36)
Torsion (degree)	8.0 ± 3.4 *	7.4 ± 4.0 **	8.6 ± 5.3	9.1 ± 4.5	13.6 ± 3.2 ††	11.8 ± 4.8
Untwisting rate (degree/sec)	-87.6 ± 36.7 *	-68.0 ± 32.1 *	-74.0 ± 32.8	-93.0 ± 36.5	-111.6 ± 27.8	-95.9 ± 33.3
CS (%)	-16.1 ± 3.8	-13.9 ± 3.5 *	-15.0 ± 3.0	-16.7 ± 2.9	-17.6 ± 2.7	-16.5 ± 3.0
CSR (1/sec)	1.68 ± 0.36	1.47 ± 0.28	1.31 ± 0.25 †	1.40 ± 0.34	1.36 ± 0.29	1.22 ± 0.21
LS (%)	-17.7 ± 2.4	-13.8 ± 2.8 * ††	-14.0 ± 3.0 *	-18.8 ± 1.6	-16.7 ± 2.1 †	-16.8 ± 2.1 †
LSR (1/sec)	2.15 ± 0.46	1.92 ± 0.36	1.76 ± 0.35	2.13 ± 0.41	1.95 ± 0.41	1.81 ± 0.27 †

TOF = Tetralogy of Fallot; LV = left ventricle; IVPD = intraventricular pressure difference; IVPG = intraventricular pressure gradient; CS = circumferential strain; CSR = circumferential strain rate; LS = longitudinal strain; LSR = longitudinal strain rate

The study population was composed of TOF patients and normal controls, and was stratified according to age group as follows: TOF1 and Control1, 4–9 years; TOF2 and Control2, 10–15 years; and TOF3 and Control3, 16–40 years. *p < 0.05 and **p < 0.001 refer to comparisons between TOF and controls from the same age group; † p < 0.05 and † † p < 0.001 refer to comparisons between TOF1 and TOF2 or TOF3, or between Control1 and Control2 or Control3; § p < 0.05 and § § p < 0.001 refer to comparisons between TOF2 and TOF3, or between Control2 and Control3.

Table 4						
Relationship between IVPGs and other parameters						
	Total IVPG		Basal IVPG		Mid to apical IVPG	
	ρ	p	ρ	p	ρ	p
Torsion (degree)		0.918	-	0.069	0.217	0.011
Untwisting rate (degree/sec)		0.626		0.205	- 0.231	0.006
CS (%)		0.078		0.762	-0.200	0.018
CSR (1/s)	0.390	< 0.001	0.440	< 0.001		0.305
LS (%)	-0.184	0.030		0.271	-0.233	0.006
LSR (1/s)	0.260	0.002	0.257	0.002	-	0.276
E (cm/sec)	0.457	< 0.001	0.503	< 0.001		0.124
e'		0.163		0.847	0.254	0.003
E/e'	0.178	0.037	0.303	< 0.001		0.212

TOF = Tetralogy of Fallot; LV = left ventricle; IVPD = intraventricular pressure difference; IVPG = intraventricular pressure gradient; CS = circumferential strain; CSR = circumferential strain rate; LS = longitudinal strain; LSR = longitudinal strain rate

Figure 1

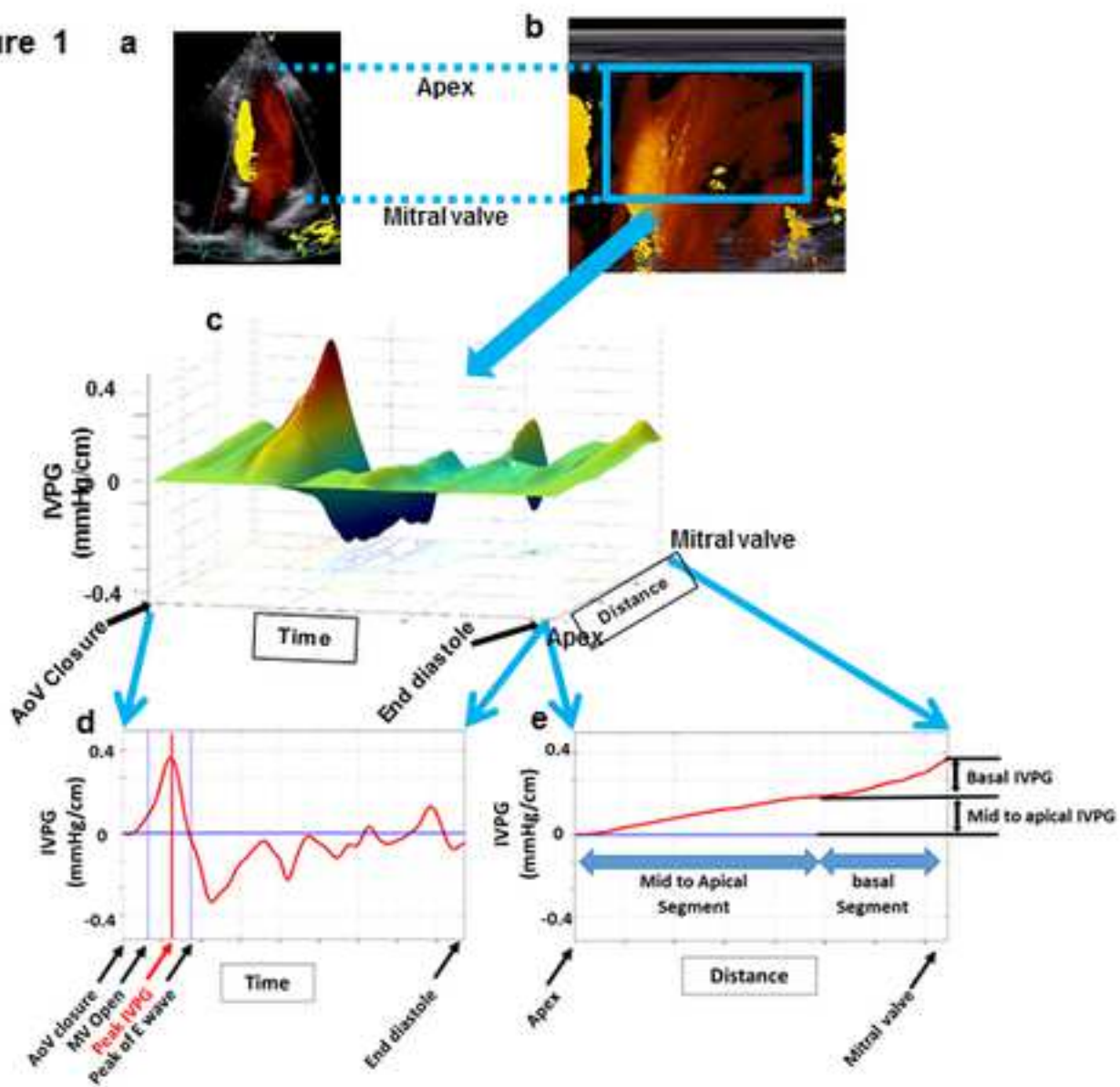


Figure 2

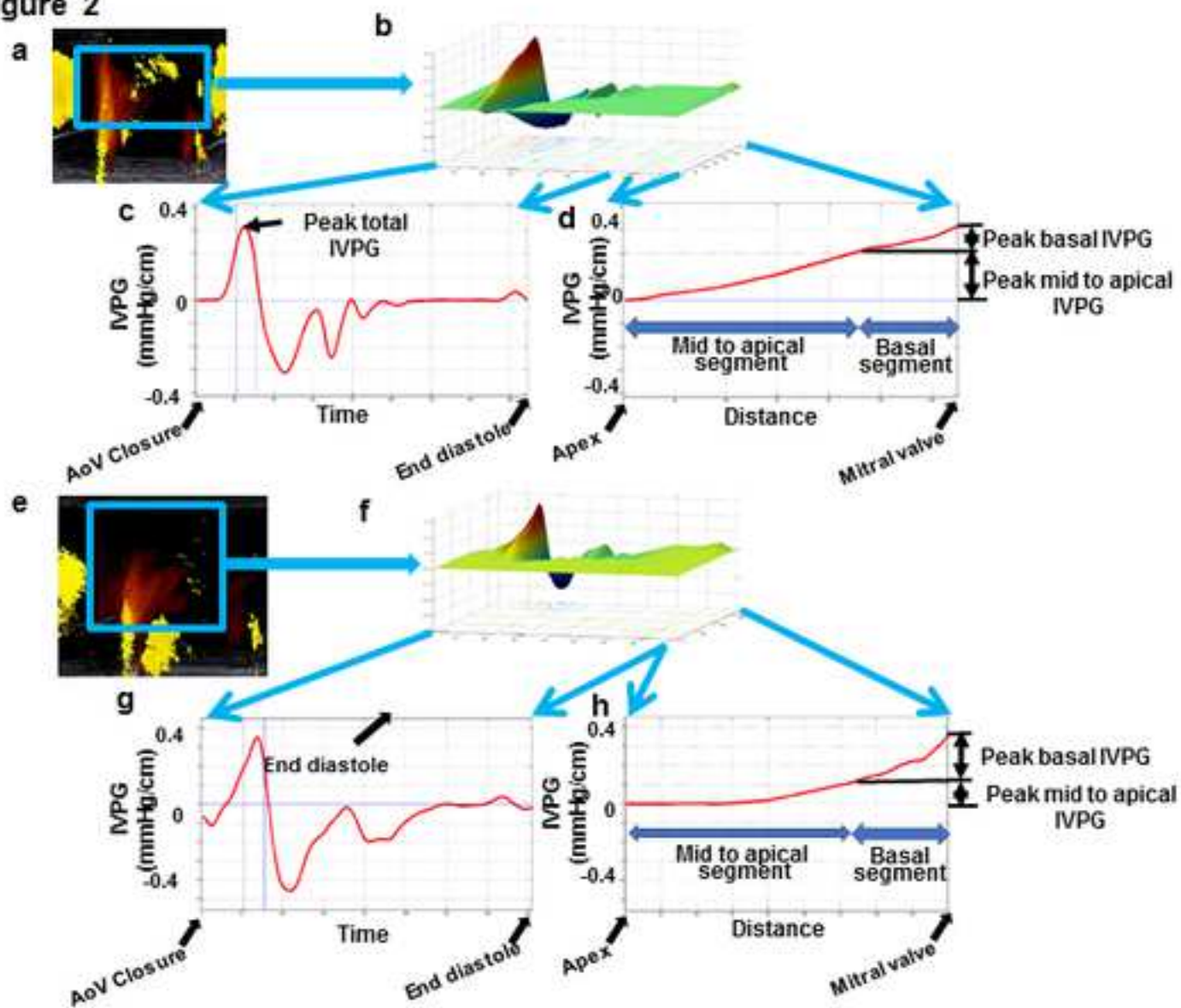


Figure 3

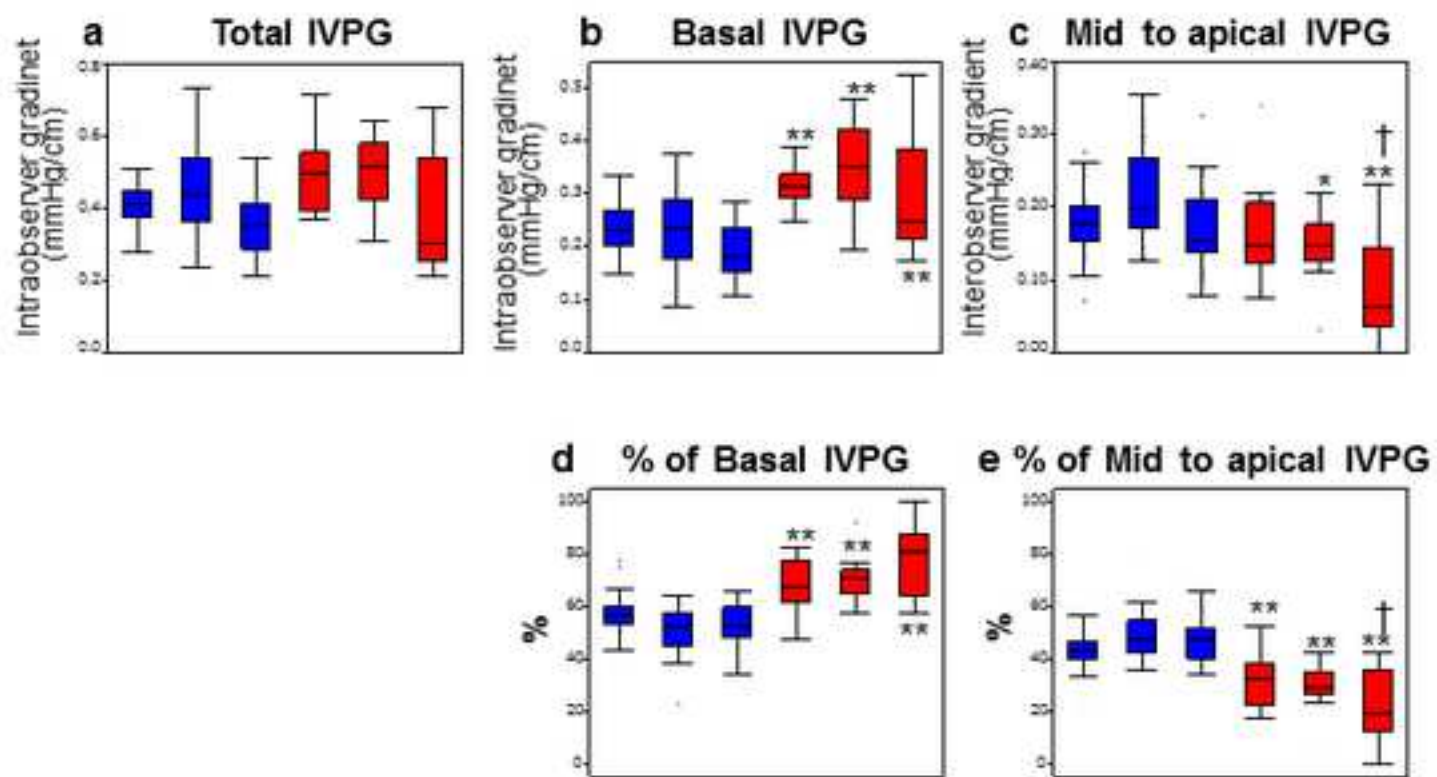
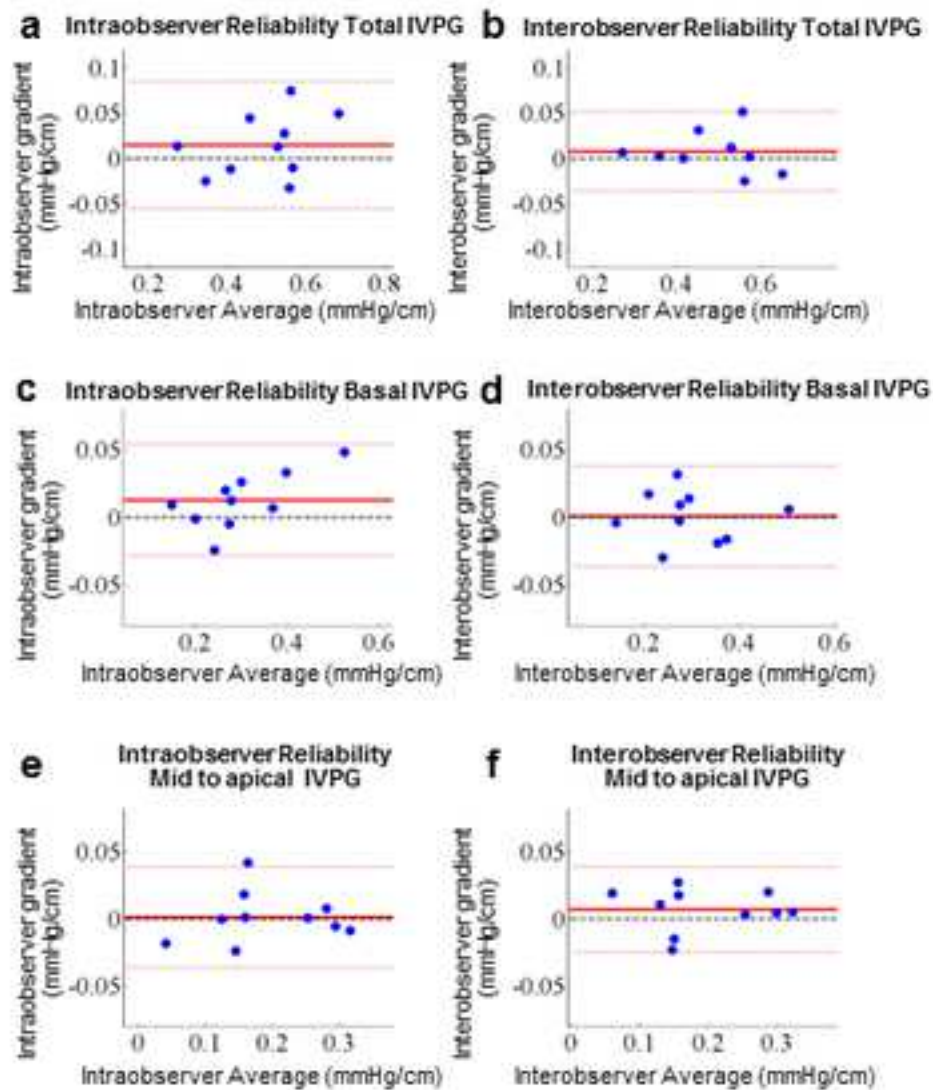


Figure 4



Supplemental table1						
IVPGs and % IVPGs						
	TOF 1 (n=12)	TOF 2 (n=13)	TOF 3 (n=13)	Control 1 (n=32)	Control 2 (n=33)	Control 3 (n=36)
Total IVPG (mmHg/cm)	0.50 ± 0.11	0.50 ± 0.10	0.38 ± 0.16	0.41 ± 0.07	0.43 ± 0.11	0.36 ± 0.08
Basal IVPG (mmHg/cm)	0.33 ± 0.08 **	0.35 ± 0.11 **	0.29 ± 0.11**	0.23 ± 0.05	0.22 ± 0.07	0.19 ± 0.05
Mid to apical IVPG (mmHg/cm)	0.16 ± 0.07	0.15 ± 0.05*	0.09 ± 0.07** †	0.18 ± 0.4	0.21 ± 0.06	0.17 ± 0.05
% of Basal IVPG (%)	68.1 ± 9.9 **	70.4 ± 8.7 **	79.2 ± 13.4**†	57.2 ± 7.6	50.7 ± 9.5	52.5 ± 8.0
% of Mid to apical IVPG (%)	31.9 ± 9.9 **	29.6 ± 8.7 **	20.8 ± 13.4** †	42.8 ± 7.6	49.2 ± 9.5	47.6 ± 8.0

TOF = Tetralogy of Fallot; IVPG = intraventricular pressure gradient

The study population was composed of TOF patients and normal controls, and was stratified according to age group as follows: TOF1 and Control1, 4–9 years; TOF2 and Control2, 10–15 years; and TOF3 and Control3, 16–40 years. *p < 0.05 and **p < 0.001 refer to comparisons between TOF and controls from the same age group; †p < 0.05 refer to comparisons between TOF1 and TOF2 or TOF3.